

# Storm Surges in the Beaufort and Chukchi Seas

Z. KOWALIK

*Institute of Marine Science, University of Alaska, Fairbanks*

Specific problems of storm surge modeling in the polar seas are analyzed. The vertically integrated equations of motion and continuity are applied to the prediction of the storm surge wave in both the ice-free and ice-covered seas. The interactions of atmosphere, ice, and water are expressed by the normal and tangential stresses. A numerical grid is set over the Chukchi and Beaufort seas, and three storm surges are simulated and briefly described. Patterns of motion and sea surface geometry are related to low and high atmospheric pressure systems. Comparison of the measured and computed sea level and observed and computed ice edge proves that the model is suitable to reproduce both water and ice motion.

## INTRODUCTION

The importance of storm surges and associated water and ice motion is related to the recent exploitation of the North Slope oil. The shore of the Beaufort Sea is generally of low relief, therefore coastal plains can be inundated by the surge and waves. The knowledge of the sea level variation along the Alaskan Beaufort and Chukchi coast is scant. Until now, tide gauges have been installed in this region for a short time only, and the present set of data is too small to estimate a statistically valid distribution of the sea level variations. Only those surges that caused extensive flooding of the coastal communities were recorded. In the eastern Beaufort Sea (Mackenzie Bay), at Tuktoyaktuk, Canada, a tide gauge was installed more than 20 years ago. Some general facts related to the storm surges in the Beaufort Sea can be inferred from this set of data. Henry [1974] analyzed storm surges in excess of  $\pm 0.9$  m for the 11-year period (1962-1973). The frequency of the major surges was not distributed uniformly in time, and the highest sea level ever recorded at Tuktoyaktuk occurred on October 4, 1963. The same surge was observed at Barrow, Alaska, one day earlier. Sea level rose 3 m above mean sea level, and this is historically the highest level ever observed at Barrow.

As a result of the lack of sea level data the range of the surge was studied by examining associated events, such as driftwood distribution. In this way, Reimnitz and Maurer [1979] found a 3-m surge along the coast of the Alaskan Beaufort Sea. They tracked the driftwood distribution caused by the storm surge in the fall of 1970. The driftwood was stranded 20 to 2000 m horizontally inshore from the mean water line. The storm occurred over the southern Beaufort Sea with winds up to 40-50 m/s. During this storm, the Tuktoyaktuk gauge was not in operation, but the setup was estimated as 3 m—even higher than the one recorded in October 1963. From Harrison Bay to MacKenzie Bay both wind and sea level were strongly correlated, and only in the vicinity of Barrow was this surge not observed.

Hunkins [1965] was probably the first to measure an open sea surge in the Chukchi Sea, when Ice Island (T-3) was aground. For 7 weeks in the spring and summer of 1961 a tide gauge was installed on Ice Island. A negative storm surge recorded on May 30, 1961, was caused by a high-pressure system, and a positive surge of about 40 cm occurred on June

18 as a result of the passage of a low-pressure system. Both pressure systems traveled from Siberia across the Chukchi Sea into the Arctic Ocean. Matthews [1971] installed recorders at Point Barrow for 3 years and was able to show seasonal variations of the surges and the presence of negative surges. These surges can produce important effects in winter, causing fracture of shorefast ice.

Wise et al. [1981] identified about 90 major storm surges around Alaska and developed a forecast procedure that is based on frequency of wind occurrence. The distribution of the wind frequency is better known through observation, but the wind is measured rarely during the storm peak. Until 1979, wind and atmospheric pressure over the Arctic Ocean were extrapolated from coastal stations and a few drifting ice stations. The possibility of modeling storm surges by applying realistic surface wind distribution was created in 1979 through the Arctic Ocean Buoy Program carried out by Thorndike and Colony [1980]. An array of buoys was placed on the ice in the Arctic Ocean to measure atmospheric pressure, air temperature, and buoy position. Storm surges usually occur together with astronomical tides, and it is essential to understand how much the surge is altered by the tide. Various measurements taken along the coasts of the Beaufort and Chukchi seas show that major surges would not be essentially altered by the tides [Huggett et al., 1975; Kowalik and Matthews, 1982]. The maximum amplitude of the tides varies from 5 to 20 cm.

In one respect, surges in the Beaufort and Chukchi seas differ from those in the mid-latitudes. The whole former area is ice covered for 8 months of the year. In summer and early autumn the southern parts of the Beaufort and Chukchi seas are ice free, and there the major storm surges are generated.

## FORMULATION OF BASIC EQUATIONS

The basis of calculations presented here will be the vertically integrated equations of water motion and continuity, written in the Cartesian coordinate system  $\{x_i\}$  with  $x_1$  directed to the east and  $x_2$  directed to the north:

$$\frac{\partial u_i}{\partial t} + \varepsilon_{ij} u_j + \frac{\partial}{\partial x_j} (u_i u_j) = -g \frac{\partial \zeta}{\partial x_i} - \frac{1}{\rho_w} \frac{\partial P_a}{\partial x_i} + \frac{(1-c)\tau_i^a}{H\rho_w} + \frac{c\tau_i^w}{H\rho_w} - \frac{\tau_i^b}{\rho_w H} + A \frac{\partial^2 u_i}{\partial x_j^2} \quad (1)$$

$$\frac{\partial \zeta}{\partial t} + \frac{\partial (H u_i)}{\partial x_i} = 0 \quad (2)$$

The ice motion induced by wind will be studied through the

Copyright 1984 by the American Geophysical Union.

Paper number 4C0866.  
0148-0227/84/004C-0866\$05.00

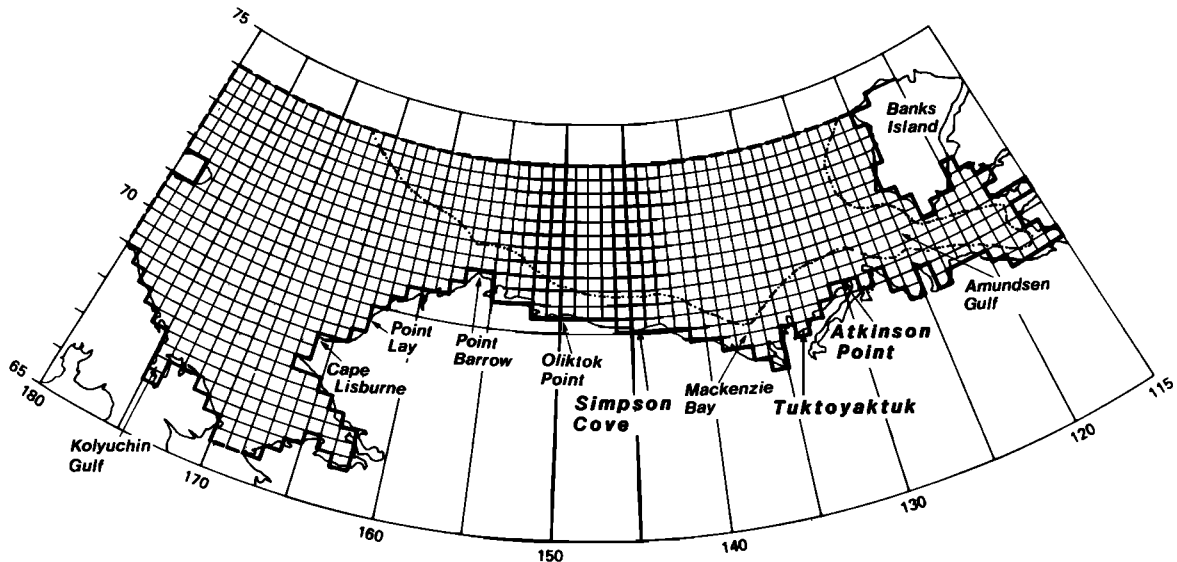


Fig. 1. Grid net for the numerical computations of the storm surges in the Beaufort and Chukchi seas: (dashed curve) open boundary; (solid curve) land boundary; (dashed-dotted curve) 200 m depth contour.

following equations of motion [Rothrock, 1975];

$$m \frac{\partial v_i}{\partial t} + m \frac{\partial}{\partial x_j} (v_i v_j) + m \epsilon_{ij} v_j = -mg \frac{\partial \zeta}{\partial x_i} - hc \frac{\partial P_a}{\partial x_i} + c(\bar{\tau}_i^a - \tau_i^w) + F_i \quad (3)$$

Rate of change of the ice mass ( $m$ ) over a specific area is equal to the net influx of mass to that area plus all sources and sinks ( $\phi$ ) [Rothrock, 1970]. The equation of continuity for the ice mass consistent with the above considerations is

$$\frac{\partial m}{\partial t} + \frac{\partial (mv_i)}{\partial x_i} = \phi \quad (4)$$

In the above equations the following notation is used:

- $i, j$  indices ( $i, j = 1, 2$ ) where 1 stands for east coordinate and 2 for west coordinate;
- $t$  time;
- $u_i$  components of the water velocity vector;
- $v_i$  components of the ice velocity vector;
- $\tau_i^a$  components of the wind stress vector over the sea;
- $\bar{\tau}_i^a$  components of the wind stress vector over the ice;
- $\tau_i^w$  components of the water stress;
- $\tau_i^b$  components of the bottom stress;
- $F_i$  components of the force resulting from internal ice stress;
- $P_a$  atmospheric pressure;

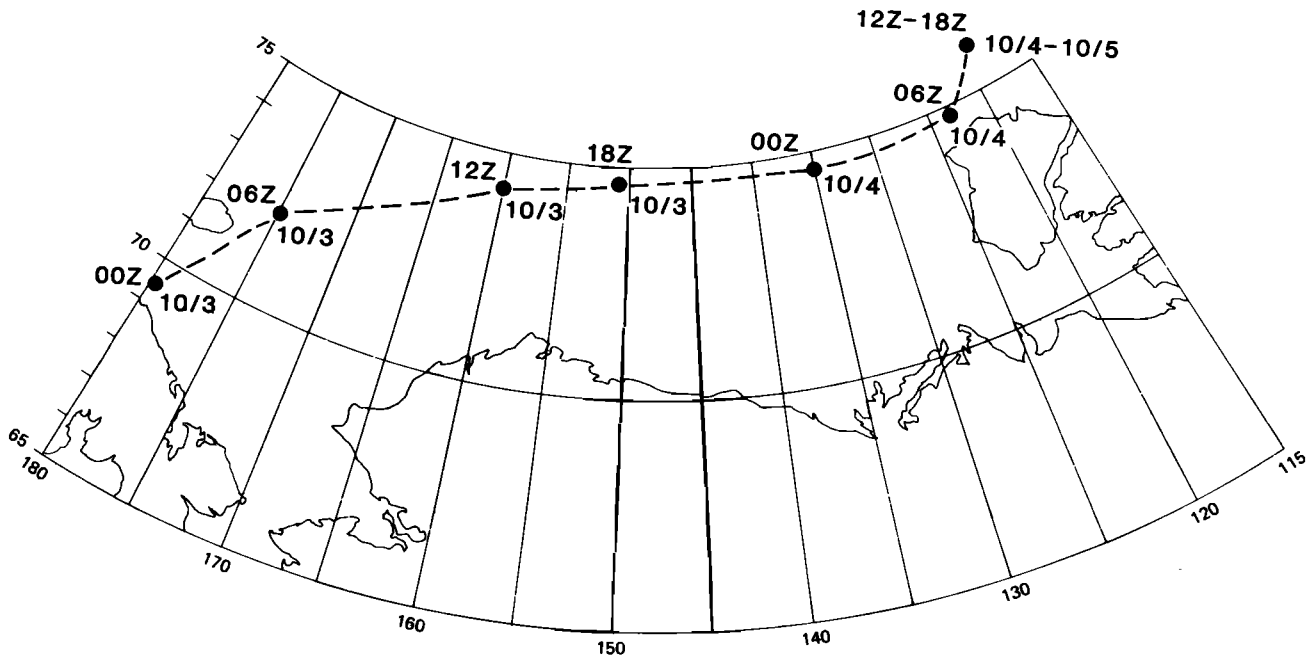


Fig. 2. Positions of the low-pressure system from 00Z, October 3, 1963, till 18Z, October 5, 1963. Dashed line represents the track of the low.

- $\epsilon_{ij}$  Coriolis tensor;
- $\zeta$  variation of the sea level or the ice around the undisturbed level;
- $c$  ice compactness,  $0 \leq c \leq 1$ ;
- $H$  water depth;
- $\rho_w$  water density;
- $A$  lateral eddy viscosity, usually will be taken as  $5 \times 10^8 \text{ cm}^2/\text{s}$ ;
- $m$  ice concentration or mass per unit area;
- $h$  ice thickness;
- $g$  gravity acceleration.

Throughout all indexed expressions, Einstein's summation convention is applied. The variables and coefficients in the equations are expressed in cgs units.

Assuming that the ice is not spread evenly over the whole sea surface, the mass of ice can be expressed through the ice compactness ( $c$ ), ice thickness ( $h$ ), and ice density ( $\rho$ ):

$$m = \rho hc \tag{5}$$

A storm surge is a phenomenon of a relatively short duration, therefore thermodynamic sources and sinks linked to  $\phi$  in (4) can be neglected. The equation of mass balance can be divided into two separate equations, i.e., a continuity equation for the ice compactness and an equation of thickness balance:

$$\frac{\partial c}{\partial t} + \frac{\partial(v_i c)}{\partial x_i} = 0 \tag{6}$$

$$\frac{\partial h}{\partial t} + v_i \frac{\partial h}{\partial x_i} = 0 \tag{7}$$

Both (4) and (6) will be applied along with (1) through (3) to obtain the ice mass and the ice compactness distributions. It is reasonable to assume that when the ice is not packed closely ( $c < 1$ ) the ice thickness is not changed as a result of the ice motion. If, on the other hand, because of internal ice stress, the ice compactness will grow beyond  $c = 1$ , the excess of compactness will lead to a change in ice thickness. In such a case the new ice thickness distribution is computed through (5).

To derive a solution to (1) through (6), suitable boundary and initial conditions must be stated. Among all possible sets of the boundary conditions the one chosen should lead to a unique solution to the above system of equations. Such a set of conditions is still undefined for the ice-ocean interaction,



Fig. 3. Wind distribution in the Beaufort and Chukchi seas for 00Z, October 5, 1963. Horizontal grid distance is scaled to 10 m/s.

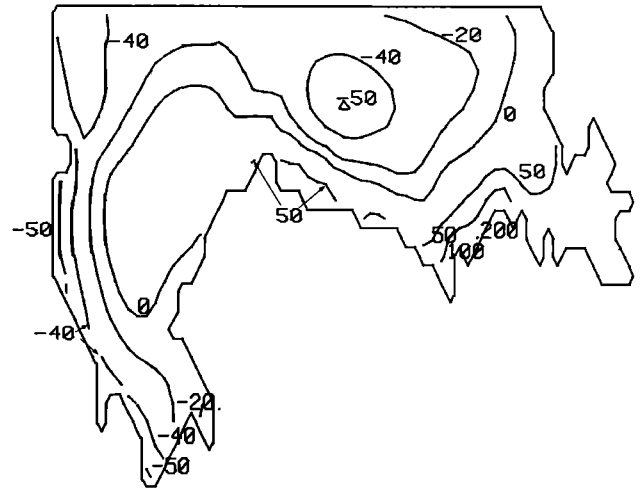


Fig. 4. Sea level distribution for 00Z, October 5, 1963. Level is given in centimeters.

therefore we shall assume (since the ice flow equations are analogous to the water flow equations) that the specification of the normal and tangential velocities along the boundaries is sufficient to derive the unique solution [Marchuk et al., 1972]. Usually, on the open boundaries (i.e., water boundaries) the storm surge velocity distribution is unknown. To overcome this hindrance, the conditions on the open boundary are specified for sea level, and instead of a parabolic problem, a new problem is formulated in which the horizontal exchange of momentum is neglected. This simplified problem is solved along the open boundary to define velocity distribution. Having defined the velocity at the boundary, the solution of the complete system of equations is sought.

SHORT DISCUSSION OF CERTAIN TERMS IN THE EQUATIONS OF MOTION

The interaction of the atmosphere, ice, and water is generally expressed through the normal and tangential stresses. The definition of the tangential stress over the ocean.

$$\tau_i^a = C_{10} \rho_a |W_i| W_i \tag{8}$$

includes the wind drag coefficient  $C_{10}$ . Recently, Garrat

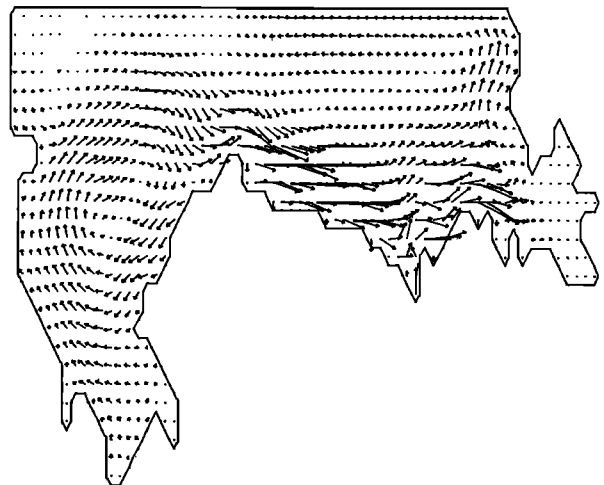


Fig. 5. Depth-averaged currents in the Beaufort and Chukchi seas for 00Z, October 5, 1963. Horizontal grid distance is scaled to 20 cm/s.

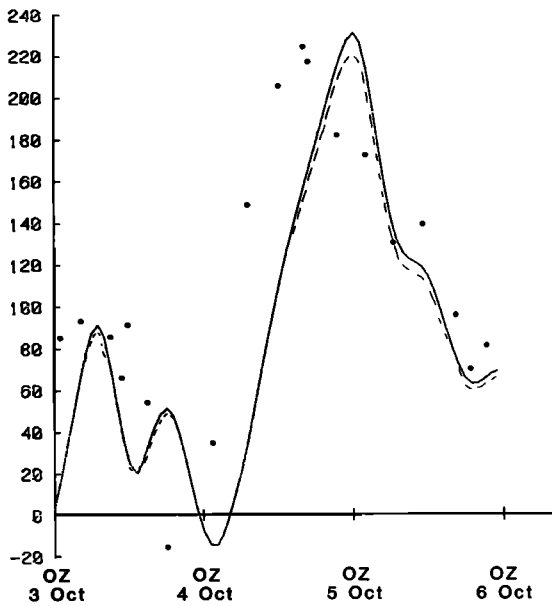


Fig. 6. Sea level variations from 00Z, October 3, 1963, till 00Z October 6, 1963, at Tuktoyaktuk, Canada: (dotted curve) measured, (dashed curve) computed with ice cover, (solid curve) computed without ice cover. Numbers are given in centimeters.

[1977] analyzed almost all measured data and found that  $C_{10}$  under a neutral atmospheric stability depends linearly on the wind velocity ( $W$ ):

$$C_{10} = (0.75 + 0.067 \times 10^{-2}W) \times 10^{-3} \quad (9)$$

where wind velocity is expressed in centimeters per second.

In practice, in storm surge computations [Henry and Heaps, 1976] the wind drag is usually set as constant and as large as  $2.7 \times 10^{-3}$ .

Definition of the wind stress over the pack ice,

$$\tilde{\tau}_i^a = \tilde{C}_{10} \rho_a |W| W_i \quad (10)$$

again leads to the same kind of problem. If one scrutinizes all

data gathered during the Arctic Ice Dynamics Joint Experiment (AIDJEX) [Pritchard, 1980] and the data dispersed in a few additional references, the dependence of  $\tilde{C}_{10}$  on wind will probably be close to the expression (9). The measurements were taken over smooth ice, which does not properly characterize the high roughness of the sea ice caused by the hummocking processes [Leavitt, 1980; McPhee, 1980]. In the ensuing computations the wind drag coefficient over the ice,  $\tilde{C}_{10}$ , will be equal to the one over the sea, i.e.,  $2.7 \times 10^{-3}$ .

Interaction of the water and ice in (1) through (7) is described by two forces: pressure gradient and water stress. The former is fully defined if sea level and atmospheric pressure are given, the latter we take as

$$\tau_i^w = \rho_w R_w |v_i - u_i| (v_i - u_i) \quad (11)$$

Water stress is sensitive both to the relative motion of the water and the ice and to the magnitude of the coefficient  $R_w$ . The water drag coefficient is a function of the hydrodynamic properties of the ice-water interface and the relative motion, its magnitude ranges from  $3 \times 10^{-3}$  to  $5.5 \times 10^{-3}$ . For the pack ice drift in summer as a result of wind, McPhee [1980] estimated the water drag magnitude to be from  $4 \times 10^{-3}$  to  $5.5 \times 10^{-3}$ . He also postulated that the ratio of the water drag coefficient to the wind drag coefficient is close to 2 ( $R_w / \tilde{C}_{10} \approx 2$ ). Since we have already chosen the wind drag coefficient, then according to this ratio,  $R_w$  will be taken as  $5.4 \times 10^{-3}$ . The water drag coefficient estimated by Langleben [1982] and by Johannessen [1970] is quite close to the above value. The drag coefficient under smooth first-year sea ice may be as small as  $1.32 \times 10^{-3}$  [Langleben, 1982].

At the sea bottom a quadratic dependence of bottom stress on the velocity is also well recognized:

$$\tau_i^b = \rho_w R |u_i| u_i \quad (12)$$

The bottom drag coefficient ( $R$ ) is a function of the bottom roughness and the properties of the bottom boundary layer [Komar, 1976].  $R$  is usually taken in the range  $2-4 \times 10^{-3}$ ; in this computation,  $R$  equals  $3 \times 10^{-3}$ .

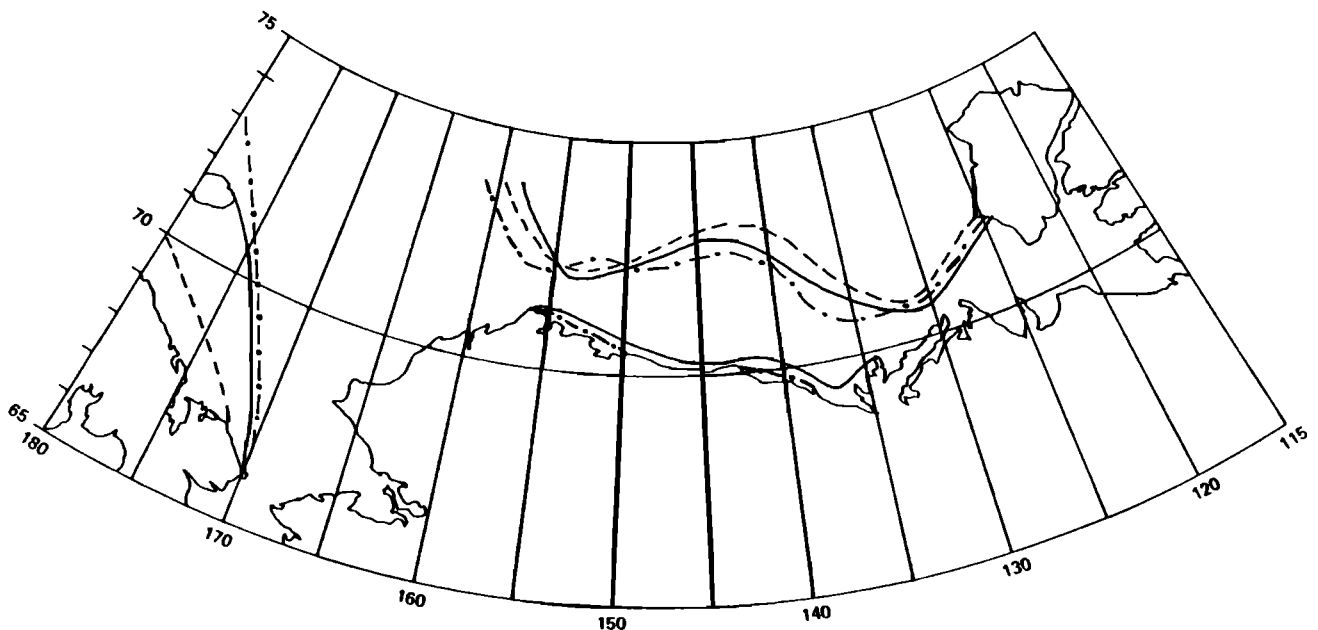


Fig. 7. Position of the ice edge: (dashed curve) observed September 26, 1979; (solid curve) observed October 7, 1979; (dashed-dotted curve) model simulation, October 7, 1979.

The important problem to be clarified before the ice-water interaction can be studied is the formulation of the constitutive law that relates the stress ( $\sigma_{ij}$ ) transmitted between floes to the variables in the problem formulated by (1) through (6). Only the mechanical behavior of ice is considered. We shall assume that during the storm surge the ice distribution will change only because of ice motion; the influence of thermodynamic processes will be neglected.

Because of internal ice stresses, the force  $F_i$  (see (3)) acts on the ice floes. The components of the force are given by the divergence of the stress tensor ( $\sigma_{ij}$ ):

$$F_i = \frac{\partial \sigma_{ij}}{\partial x_j} m \tag{13}$$

We have experimented with the few available constitutive laws to express the ice mechanics, i.e., an elastic constitutive law developed by *Ovsienko* [1976]; the viscous and elastic model of *Rothrock* [1975]; and the viscous model of *Glen* [1970]. Treatment of the pack ice as an elastic-plastic or as a viscous-elastic material brings into consideration the additional variables not specified in the system (1)-(6). Application of the nonlinear viscous constitutive law can set results that are difficult to test critically against the measurements [Kowalik, 1981]. Therefore, in the ensuing computations the linear viscous model will be applied; in that case the ice stress is proportional to the strain rate tensor, and the internal force becomes

$$F_i = \eta \frac{\partial^2 v_i}{\partial x_j \partial x_j} m \tag{14}$$

The magnitude of the kinematic viscosity coefficient ( $\eta$ ) is difficult to evaluate. In the Arctic Ocean and in the Weddell Sea, *Campbell* [1965] and *Ling et al.* [1980] found the coefficients by tuning the computed pattern of the mean ice circulation to the observed pattern. The estimated values ranged from  $5 \times 10^{10}$  to  $5 \times 10^{12}$  cm<sup>2</sup>/s. To evaluate the influence of viscosity on tidal waves, a sequence of investigations was carried out by *Kowalik* [1981] in the Arctic Ocean. The viscosity coefficients found for the steady motions when applied to the tide led to the suppression of the tide and, therefore, are unsuitable to describe time-dependent motion.

Closer to the natural conditions is the assumption that the

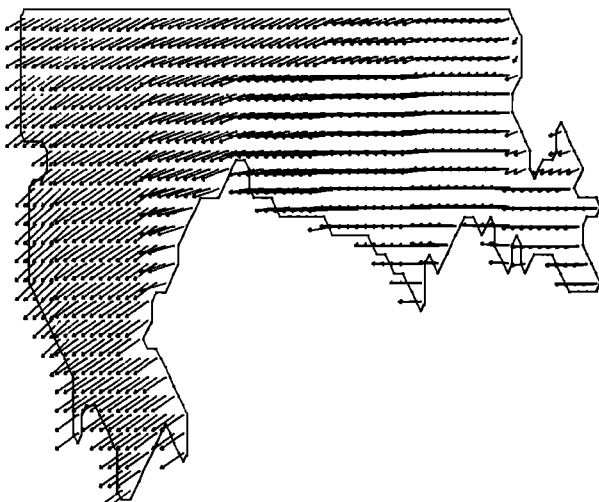


Fig. 8. Wind distribution for 12Z, October 3, 1979. Horizontal grid distance is scaled to 5 m/s.

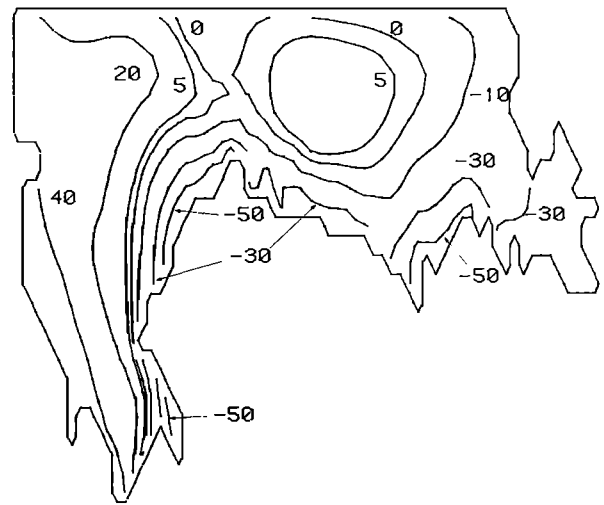


Fig. 9. Sea level distribution for 12Z, October 3, 1979. Numbers are given in centimeters.

viscosity coefficient is a function of the ice compactness. Linear dependence proposed by *Doronin* [1970]

$$\eta = \alpha c \quad \alpha \approx 5 \times 10^{10} \text{ cm}^2/\text{s} \tag{15}$$

proved to be valuable in the prediction of the ice drift.

The applied constitutive law contains rather simple mechanical properties of the ice, but it seems to describe the interaction of a storm surge or tide with the pack ice in a satisfactory manner. For the long period processes, sophisticated models of the ice floe interaction, with both mechanical and thermodynamical properties have been proposed by *Coon et al.* [1974] and *Hibler* [1979].

#### NUMERICAL MODELING: AREA, GRID, AND BOUNDARY CONDITIONS

Two previous efforts to model the storm surges in the Beaufort and Chukchi seas must be mentioned. *Schafer* [1966] computed surge distribution at Barrow by simulating the storm surge of October 3, 1963. *Henry and Heaps* [1976] applied numerical methods to the storm surges in the southern Beaufort Sea. Both models were based on the vertically inte-

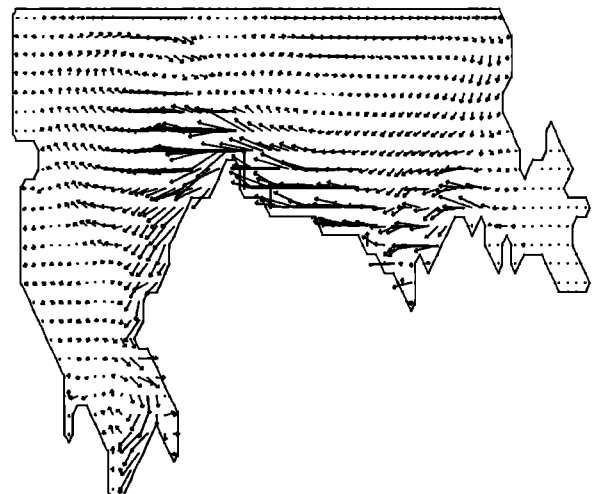


Fig. 10. Depth-averaged currents for 12Z, October 3, 1979. Horizontal grid distance is scaled to 10 cm/s.

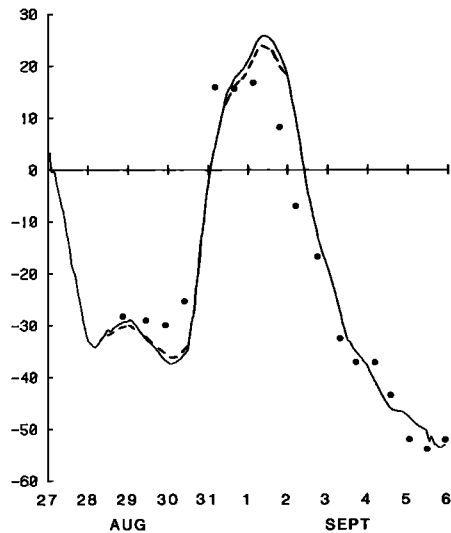


Fig. 11. Sea level changes from 00Z, August 27, 1981, till 00Z, September 6, 1981, at Simpson Cove, Alaska: (dotted curve) measured, (dashed curve) computed with ice cover, (solid curve) computed without ice cover. Numbers are given in centimeters.

grated equations of motion and continuity (1) and (2), but the influence of ice cover was neglected.

We shall study the storm surge generation and propagation by applying the full system of equations (1)–(6). To solve this set of equations, an explicit-in-time and staggered-in-space numerical scheme will be applied after Hansen [1962]. The influence of the ice cover on the stability conditions of this scheme has been studied by Kowalik [1981]. To include ice into the storm surge model, it was assumed that variations of the pack ice distribution are due entirely to the wind and not to the thermodynamical processes. The assumption is based on Wendler's [1973] analysis of actual summer situation for the 5-day periods in the Beaufort Sea. He was able to show that the ice conditions were strongly correlated to the wind direction.

The responses of the sea level to the storm passages will be considered in the domain depicted in Figure 1. Because of the large dimension of the area, the spherical shape of the earth cannot be neglected, and therefore a spherical system of coordinates is introduced to the system of equations (1)–(6). The grid intervals of numerical lattice in Figure 1 are  $1/3$  of a degree of latitude and 1 degree of longitude, i.e., at latitude  $70^\circ\text{N}$  the grid length is about 38 km. The open boundary follows the  $74^\circ\text{N}$  parallel from Banks Island to  $180^\circ\text{W}$ , then south along this meridian to the Siberian coast; the second open boundary is set in the Bering Strait. To derive a unique solution to equations (1)–(6), both initial and boundary conditions must be specified. On the open boundary (for the water) a radiating condition proposed by Reid and Bodine [1968] is selected. It allows for any long wave propagating from the interior to pass freely through the boundary. A few experiments have been carried out with zero level at the open boundary. This condition leads to the different patterns of the surge in the vicinity of the open boundary, but the surge at the coast is usually quite similar to the case when sea level is defined by open radiating condition. Usually, sea level changes substantially at the shore and over the shallow water area, therefore if the open boundary condition is set beyond shelf, its influence on the surge distribution at the coast should be insignificant. The condition of zero elevation can be readily applied to the southern Beaufort Sea, where the shelf is

narrow and the largest depth is about 4 km. The application of this condition in the Chukchi Sea area is a moot question because almost everywhere the depth is less than 200 m, and even at large distances from the shore a strong sea level variation can be generated. Both conditions set the solutions along the open boundary that display certain levels of distortion when compared against a solution of the complete problem or against a solution in which the open boundary has been moved away from the previous location. Certainly, the normal velocity to the open boundary in the Beaufort Sea (Figure 5) seems to be very small, thus the flow is parallel to the open boundary.

Open boundary conditions for the ice velocity and compactness are not easily specified. One set of conditions can be defined by assuming continuity of the ice velocity and compactness across the boundary and setting first and second derivatives equal to zero. This condition, though numerically feasible, assumes that the motion in the domain is defined completely by internal processes and is not influenced by the motion from outside the domain. Such an approach is appropriate for the storm surges, when open boundary condition is set beyond the shelf, but whether it is appropriate for the ice motion remains to be proven. An alternative set of boundary conditions can be determined by the measurements from the buoys deployed in the Arctic Ocean in the proximity of the boundary during simulated storm surge. In reproducing the storm surge from 1979, both boundary conditions, i.e., measured ice velocity and continuity of velocity and its derivatives, were employed. Probably as a result of the short time of the storm surge, the ice distributions in both cases were quite similar. Modeling of the ice movement with the open boundary still requires additional measurements to critically test the model output.

#### MODELING OF THE STORM SURGES IN THE BEAUFORT AND CHUKCHI SEAS

##### Storm Surge of October 1963

Meteorological observations at the time of the storm were very scant. Surface pressure maps from the Canadian

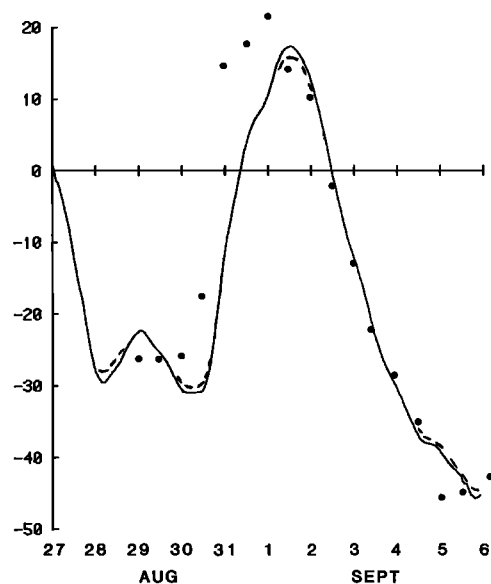


Fig. 12. Sea level changes from 00Z, August 27, 1981, till 00Z, September 6, 1981, at Demarcation Bay: (dotted curve) measured, (dashed curve) computed with ice cover, (solid curve) computed without ice cover. Numbers are given in centimeters.

Meteorological Centre for the 6-hour intervals allowed reconstruction of the storm track (Figure 2). One has to understand that the numbers given on the maps are extrapolated from the few coastal stations. Our work was greatly facilitated by weather analysis of the storm performed by *Schafer* [1966].

The low-pressure center traveled from Siberia (00Z, October 3) to the northern shores of Banks Island (06Z, October 4), where it stayed for about 24 hours. The low on its way was a source of unusually strong winds. Record high surges of about 3 m were reported along the Alaskan coast of the Chukchi Sea [Schafer, 1966], and a very high surge of about 2 m was recorded in Tuktoyaktuk at the eastern coast of Mackenzie Bay. In both cases the high surges were due to the northwest winds, and it is obvious that the direction of the shoreline in both areas is quite similar. An additional factor that might have influenced the sea level in Chukchi Sea was the high velocity of the pressure center. The center traveled a distance of about 2100 km in 30 hours, with an average velocity of about 19.5 m/s. The velocity of the long free waves, defined as  $c = \sqrt{gH}$ , is quite large in the Beaufort Sea because of the large depth, but in the Chukchi the average depth is about 50 m, therefore the velocity of the long wave is 22 m/s. Because the velocity of the atmospheric pressure center in the Chukchi Sea was close to the velocity of the free waves, the large sea level variations can be related to the resonance effects [Lamb, 1945].

Every 6 hours, starting 00Z October 3 until 00Z October 6, the wind distribution was computed from the surface pressure maps. Between 6-hour readings, the wind velocity was interpolated linearly in time. To compute geostrophic winds, the region was subdivided into lattices of 2° latitude and 10° longitude, and pressure was taken in the grid points. Based on the data gathered during the AIDJEX experiment [Albright, 1980], in computing surface wind distribution, the cross-isobar turning angle ( $\alpha = 24^\circ$ ) and the ratio of the surface wind ( $W$ ) to the geostrophic wind ( $G$ ),  $W/G = 0.6$ , were applied.

Usually, two types of computations were attempted. First, the sea surface was assumed to be ice free, and only equations

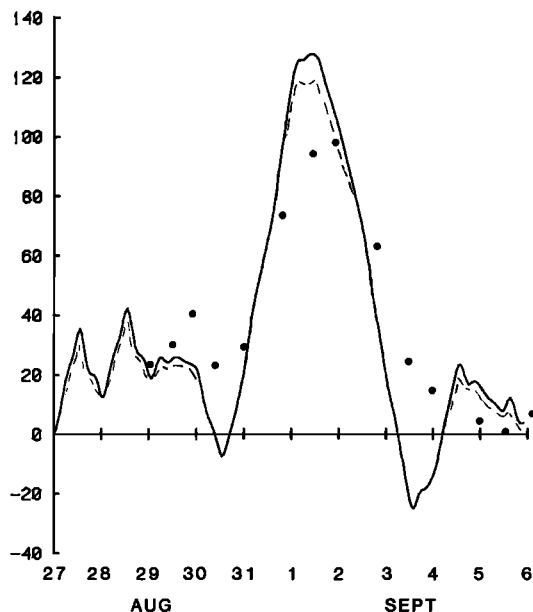


Fig. 13. Sea level changes from 00Z, August 27, 1981, till 00Z, September 6, 1981, at Tuktoyaktuk, Canada: (dotted curve) measured, (dashed curve) computed with ice cover, (solid curve) computed without ice cover. Numbers are given in centimeters.

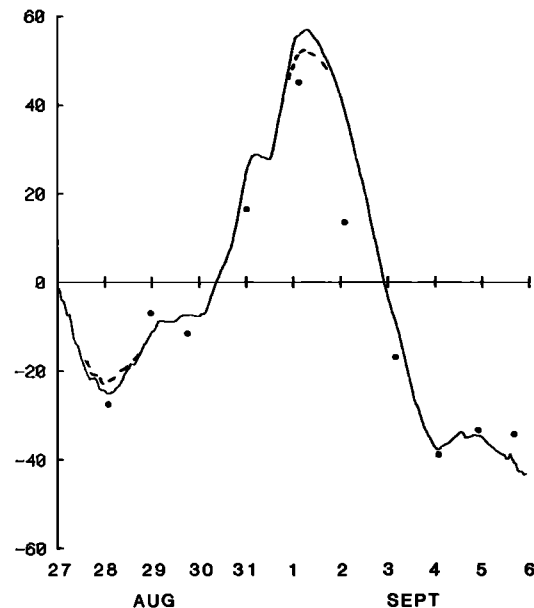


Fig. 14. Sea level variations from 00Z, August 27, 1981, till 00Z, September 6, 1981, at Atkinson Point, Canada; (dotted curve) measured, (dashed curve) computed with ice cover, (solid curve) computed without ice cover. Numbers are given in centimeters.

describing water motion were applied. In the second case the actual ice distribution has been taken as the initial condition, and the storm surge was computed by applying the complete set of equations of ice and water motion. By comparing two simulations, one can conclude that even an ice cover of about 4/10 is practically equivalent to the open water when storm surge generation or propagation is studied. Because available sea level data are related to the storm surges that occurred during fall or late summer, when the nearshore compactness was less than 0.4, we do not have data to test critically the model against higher ice compactness.

To represent a typical pattern of the sea level and current during the storm, the situation on October 5, 00Z, will be described. The low-pressure center was situated to the north from Banks Island, and only in the Mackenzie Bay area the northwest wind (Figure 3) set sea level about 2 m above the mean sea level (Figure 4). Sea level displays a characteristic pattern, which often occurs in the major surges. Both in the Beaufort and Chukchi seas, the sea level contours away from the shore tend to develop domelike structures. According to the geostrophic flow pattern, the velocity vectors tend to be parallel to the sea level contour lines. Two domes in the sea level structure divide the flow into two large gyres (Figure 5). The division line runs from Point Barrow to the north. The maximum setup observed during the storm at Barrow on October 4, 00Z, compares quite well with the 2.5-m surge obtained by modeling. Temporal dependence of the measured sea level in Tuktoyaktuk, against the computed values, is given in Figure 6.

#### Negative Surges: Open Water Season 1979

During the open water season of May to November 1979, a tide gauge was deployed by Outer Continental Shelf Environmental Program in Harrison Bay. As a result of ice conditions the three tide gauges in Canada were not in operation during the storm. Storm surges occurred in September and October, and all major surges were negative. A negative surge of about 50 cm from September 26 to October 7 is reproduced. The

storm was due to an atmospheric high-pressure system with the center situated between Point Barrow and the North Pole [Thorndike and Colony, 1980]. This is a typical weather situation that generates patterns of ice and surface water motion often observed through the ice drift and is responsible for the so-called Beaufort Gyre. The pressure systems during the storm of 1979 occupied nearly the same position for about 10 days. Based on the geostrophical wind computation, east and northeast winds from 7 to 15 m/s were found. Again, two sets of experiments were run, i.e., with and without an ice cover. To describe the wind influence on the ice distribution, the position of the ice edge at the start and end of the storm, as observed by the satellite, is plotted (Figure 7). Ice edge position on October 7, computed by model, is also plotted in the same figure. Both computed and observed positions of the ice edge along the Siberian coast show its movement toward the east. Initially, ice cover along the Beaufort coast was negligible, but the east and northeast wind piled pack ice against the shore. During computation, the ice compactness of 0.4 defined the position of the ice edge.

For the period September 26 to October 7 the wind direction was practically constant, thus after a few days the flow and sea level pattern was quasi-steady. The wind, current, and sea level at the peak of the storm on October 3, 12Z, is described in Figures 8, 9, 10. Throughout the whole period both current and sea level show a consistent distribution related to the wind. Strong currents and sea level variations again occurred in the shallow coastal area. After about 3–4 days, along the shelf from Mackenzie Bay to Point Barrow, a current somewhat reminiscent of a "coastal jet" [Csanady, 1974] develops. In the vicinity of Barrow, probably as a result of the shape of the shoreline and the depth difference between the Beaufort and Chukchi seas, the coastal current partly branches off into open water and partially follows the coastal contour into the Chukchi Sea. This division line again splits the motion into two gyres, which are closely associated with the dome structure of the sea level. Because the direction of the current in the gyres is related to the sea level distribution, it is only in the initial period of the wind action that the current at the sea surface can be associated with the wind. After the initial period, the sea level variations can alter the dynamics of the flow conspicuously.

#### *Storm Surge, August 30–September 1, 1981*

Near the end of August 1981, a low-pressure center moved southward along the Canadian Islands from the high-latitude region. For 2–3 days the low maintained strong northwest winds over the eastern Beaufort Sea. According to the *Beaufort Weather and Ice Office* [1981], it was the second longest storm of the season, with wind speeds up to 40 knots. While the eastern and central Beaufort Sea was under the influence of the strong low, the winds over the Chukchi and western Beaufort seas were due to the shallow high with its center over Siberia. In August and September 1981, 11 tide gauges were installed along the Beaufort coast both in the United States and Canada. A positive surge of about 60 cm was recorded in the Canadian Beaufort Sea. Toward the west, the surge was mixed; it was negative at the beginning and changed to positive when winds changed their direction to northwest. The storm occurred between August 30 and September 1, 1981, only, but to study the whole process, the computation was extended for 10 days: from August 27, 00Z, to September 6, 00Z. Again, to compute the temporal and spatial distribution of the wind, the data compiled by Thorndike et al. [1982] were

used. Unfortunately, the atmospheric pressure was only available for 12-hour intervals. For comparison with computed sea level the four tide gauges along the Beaufort coast were used (Figures 11–14). The measured level compares quite well with computed sea level. The low temporal resolution of the wind field is the probable cause of a time lag between the calculated and recorded maximum of the sea level. As in the previous computations the sea level chart (not shown) displays two domes, and in the current distribution, two gyres are observed.

#### CONCLUSION

The vertically integrated system of equations proved long ago to be very effective in the prediction of sea level and mean currents. We have attempted the same approach to combined water and ice motion. Although only the open water seasons, conducive to storm generation, were considered, the results are encouraging. Modeling of the ice motion with an open boundary requires further comparison with observation under various boundary conditions until a reliable approach can be established.

Results from the storm surge computations display the relationships of the sea level and current distribution. Because of the depth and shoreline geometry, the pattern of motion in the Beaufort Sea is quite different from that in the Chukchi Sea. In both basins the storm surge tends to develop a dome structure in the sea level distribution. Velocity tends to be parallel to the sea level contours according to the geostrophic adjustment, therefore two gyres are observed in which motion takes place around the domes. In the Chukchi Sea, both current and sea level display strong variations not only at the shore but at large distances from the coast as well. In the Beaufort Sea the changes are usually confined to the nearshore region. During major surges, a coastal current develops along the shelf from Mackenzie Bay to Point Barrow. The results of computation close to the northern boundary should be taken cautiously because they might be distorted by the open boundary condition.

All numerical simulations were done for the ice-free and ice-covered sea surface, but the influence of the ice was practically negligible because major surges took place in summer and fall when the Chukchi and Beaufort seas were only partly covered by ice.

*Acknowledgments.* This study was funded wholly by the Mineral Management Service, through interagency agreement with the National Oceanic and Atmospheric Administration, as part of the Outer Continental Shelf Environmental Program. I would like to express my gratitude to A. Thorndike (Polar Science Center, University of Washington) for his help in preparing the atmospheric pressure data for the wind calculation and in discussing the air-ice interaction problems. I am grateful to D. Bain (State of Alaska, Department of Natural Resources), B. Matthews (University of Alaska, Fairbanks), F. E. Stephenson (Institute of Ocean Sciences, Sidney, Victoria, B. C.), J. and Nasr (Fisheries and Oceans, Ottawa) for offering me unpublished data on the sea level variations in the Chukchi and Beaufort seas. I am greatly indebted to M. Pelto (OCS, Juneau) and G. Weller (University of Alaska, Fairbanks), colleagues within the Institute of Marine Science, University of Alaska, for their help and discussions throughout the work and to the reviewers for their constructive comments. This paper is contribution 549 of the Institute of Marine Science, University of Alaska, Fairbanks.

#### REFERENCES

- Albright, M., Geostrophic wind calculations for AIDJEX, in *Sea Ice Processes and Models*, edited by R. S. Pritchard, 474 pp., University of Washington Press, Seattle, 1980.

- Beaufort Weather and Ice Office, 1981 Report, 172 pp., Atmos. Environ. Serv. West. Reg., Arctic Weather Center, Edmonton, Canada, 1981.
- Campbell, W. J., The wind-driven circulation of ice and water in a polar ocean, *J. Geophys. Res.*, 70(14), 3279–3301, 1965.
- Csanady, T. T., Barotropic currents over the continental shelf, *J. Phys. Oceanogr.*, 4(3), 357–371, 1974.
- Coon, M. D., G. A. Maykut, R. S. Pritchard, D. A. Rothrock, and A. S. Thorndike, Modeling the pack ice as an elastic-plastic material, *AIDJEX Bull.*, 24, 1–105, 1974.
- Doronin, Yu. D., On the method of calculate compactness and drift ice, *Tr. Arctic-Antarctic Inst.*, 291, 5–17, 1970.
- Garrat, J. R., Review of drag coefficients over oceans and continents, *Mon. Weather Rev.*, 7(105), 915–929, 1977.
- Glen, J. W., Thoughts on a viscous model for sea ice, *AIDJEX Bull.*, 2, 18–27, 1970.
- Hansen, W., Hydrodynamical methods applied to the oceanographical problems, Proceedings of the Symposium on Mathematical-Hydrodynamical Methods in Physical Oceanography, *Mitt. Inst. Meeresk., Univ. Hamburg*, 1, 25–34, 1962.
- Henry, R. F., Storm surges in the southern Beaufort Sea, interim report, 14 pp., Beaufort Sea Proj., Inst. Ocean Sci., Patricia Bay, Sidney, B.C., Can., 1974.
- Henry, R. F., and N. S. Heaps, Storm surge in the southern Beaufort Sea, *J. Fish. Res. Board Can.*, 33(10), 2362–2376, 1976.
- Hibler, W. D., III A dynamic-thermodynamic sea ice model, *J. Phys. Oceanogr.*, 9, 815–846, 1979.
- Huggett, W. S., M. J. Woodward, F. Stephenson, F. V. Hermiston, and A. Douglas, Near bottom currents and offshore tides, *Tech. Rep. 16*, 38 pp., Beaufort Sea Proj., Inst. Ocean Sci., Sidney, B.C., Can., 1975.
- Hunkins, K. L., Tide and storm surge observations in the Chukchi Sea, *Limnol. Oceanogr.*, 10, 29–39, 1965.
- Johannessen, O. M., Note on some vertical current profiles below ice floes in the Gulf of St. Lawrence and near the North Pole, *J. Geophys. Res.*, 75, 2857–2862, 1970.
- Komar, P. D., Boundary layer flow under steady unidirectional currents, in *Marine Sediment Transport and Environmental Management*, edited by D. J. Stanley and D. J. P. Swift, pp. 91–106, John Wiley, New York, 1976.
- Kowalik, Z., A study of  $M_2$  tide in the ice-covered Arctic Ocean, *Modeling Identification and Control*, 2(4), 201–223, 1981.
- Kowalik, Z., and J. B. Matthews, The  $M_2$  tide in the Beaufort and Chukchi seas, *J. Phys. Oceanogr.*, 12(7), 743–746, 1982.
- Lamb, H., *Hydrodynamics*, 738 pp., Dover, New York, 1945.
- Langbein, M. P., Water drag coefficient of the first-year sea-ice, *J. Geophys. Res.*, 87(1), 573–578, 1982.
- Leavitt, E., Surface-based air stress measurements made during AIDJEX, in *Proceedings of the AIDJEX Symposium*, edited by R. S. Pritchard, pp. 419–429, University of Washington Press, Seattle, 1980.
- Ling, C. H., L. A. Rasmussen, and W. J. Campbell, A continuum sea ice model for a global climate model, in *Proceedings of the AIDJEX Symposium*, edited by R. S. Pritchard, pp. 187–196, University of Washington Press, Seattle, 1980.
- Marchuk, G., R. Gordev, B. Kagan, and V. Rivkind, Numerical method to solve tidal dynamics equation and results of its testing, report, 78 pp., Comput. Centre. Novosibirsk, U.S.S.R., 1972.
- Matthews, J. B., Long period gravity waves and storm surges on the Arctic Ocean continental shelf, paper presented at Proceedings of Joint Oceanographic Assembly, Tokyo, 1971.
- McPhee, M. G., An analysis of pack ice drift in summer, in *Proceedings of the AIDJEX Symposium*, pp. 62–75, University of Washington Press, Seattle, 1980.
- Ovsienko, S. N., On the numerical modelling of the ice drift, *Izv. Atmos. Oceanic Phys.*, 12(11), 1201–1206, 1976.
- Pritchard, R. S. (Ed.), Sea ice and models, *Proceedings of the AIDJEX Symposium*, 474 pp., University of Washington Press, Seattle, 1980.
- Reid, R. O., and B. R. Bodine, Numerical model for storm surges in Galveston Bay, *J. Waterway Harbour Div.*, 94(WWI), 33–57, 1968.
- Reimnitz, F., and D. K. Maurer, Effect of storm surge on the Beaufort Sea coast, northern Alaska, *Arctic*, 32, 329–344, 1979.
- Rothrock, D. A., The kinematics and mechanical behaviour of pack ice: the state of subject, *AIDJEX Bull.*, 2, 1–10, 1970.
- Rothrock, D. A., The mechanical behaviour of pack ice, *Ann. Rev. Earth Planet. Sci.*, 3, 317–342, 1975.
- Schafer, P. J., Computation of a storm surge at Barrow, Alaska, *Archiv. Meteorol., Geophys. Bioklimatol. A*, 15(3–4), 372–393, 1966.
- Thorndike, A. S., and R. Colony, Arctic Ocean Buoy Program, data report, 131 pp., Polar Sci. Center, Univ. Wash., Seattle, 1980.
- Thronkike, A. S., R. Colony, and E. A. Muñoz, Arctic Ocean Buoy Program, data report, 137 pp., Polar Sci. Center, Univ. Wash., Seattle, 1982.
- Wendler, G., Sea ice observation by means of satellite, *J. Geophys. Res.*, 78(9), 1427–1448, 1973.
- Wise, J. L., A. L. Comiskey, and R. Becker, Storm Surge Climatology and Forecasting in Alaska, 26 pp., Arctic Environ. Inform. Data Center, Anchorage, 1981.

Z. Kowalik, Institute of Marine Science, University of Alaska, Fairbanks, AL 99701.

(Received March 16, 1984;  
accepted May 14, 1984.)